Geomagnetic Survey of the Compass Swing Testing Site at Nelson Airport

5 August 2019

Cassandra Trinh-Le and Steven Kesler

School of Geography, Environment and Earth Sciences
Victoria University of Wellington
New Zealand

1. Summary

A survey of Total Magnetic Field Intensity (*TF*) was conducted across the compass swing testing site at Nelson Airport on 2 July 2019, in accordance with the requirements stipulated in the Civil Aviation Authority Advisory Circular AC43-7 Revision 1 (CAA AC43-7). The variation in *TF* anomaly across the site was 8.06 nT, equivalent to a maximum possible horizontal deviation of magnetic North by 0.026°; this is 26% of the permissible deviation of 0.1° for a CAA AC43-7 Class 1 site. This result confirms that the Nelson Airport compass swing testing site qualifies as a Class 1 site.

2. Introduction

The Victoria University of Wellington School of Geography, Environment and Earth Sciences was approached by Air Nelson to perform a geomagnetic survey of the compass swing testing site at Nelson Airport. This is the second of the 5-yearly resurveys that are mandated in the Civil Aviation Authority Advisory Circular AC43-7 Revision 1 (CAA, 2000; hereafter AC43-7). The initial magnetic survey of the site (Henderson and Bourguignon, 2007) found that Total Magnetic Field Intensity (*TF*) varied by ~7 nT across the area, equivalent to ~22.5% of the permissible 31 nT for the Nelson region as specified in AC43-7; the testing site was therefore rated as Class 1.

3. Survey location and method

The Nelson Airport compass swing testing site is located near the southern end of the main aircraft taxiway (Figure 1). The site is a 53.5 by 57.6 m area oriented parallel to the taxiway. *TF* observations were made on a 12 by 13 grid of points (156 points) covering the entire testing area (see Appendix I). The grid spacing was 5 ± 0.1 m, with smaller spacings along the western and southern sides to ensure complete coverage. The density of survey points exceeds the requirements set forth in AC43-7.

The grid points were measured and marked on the ground with spray paint by Air Nelson engineers (approximately 20 minutes set up time), and then the magnetic survey was conducted between 11:44 am and 2:16 pm on 2 July 2019 (NZT). Repeat readings were made at the base station [grid point (0, 0)] at the end of each traverse to determine a correction for time-varying components of the geomagnetic field (see 3.2 and Appendix II). Due to being on an active runway, the survey was paused intermittently to allow planes to taxi by, and the runway lights were turned off for the duration of the survey to minimise electrical disturbance.

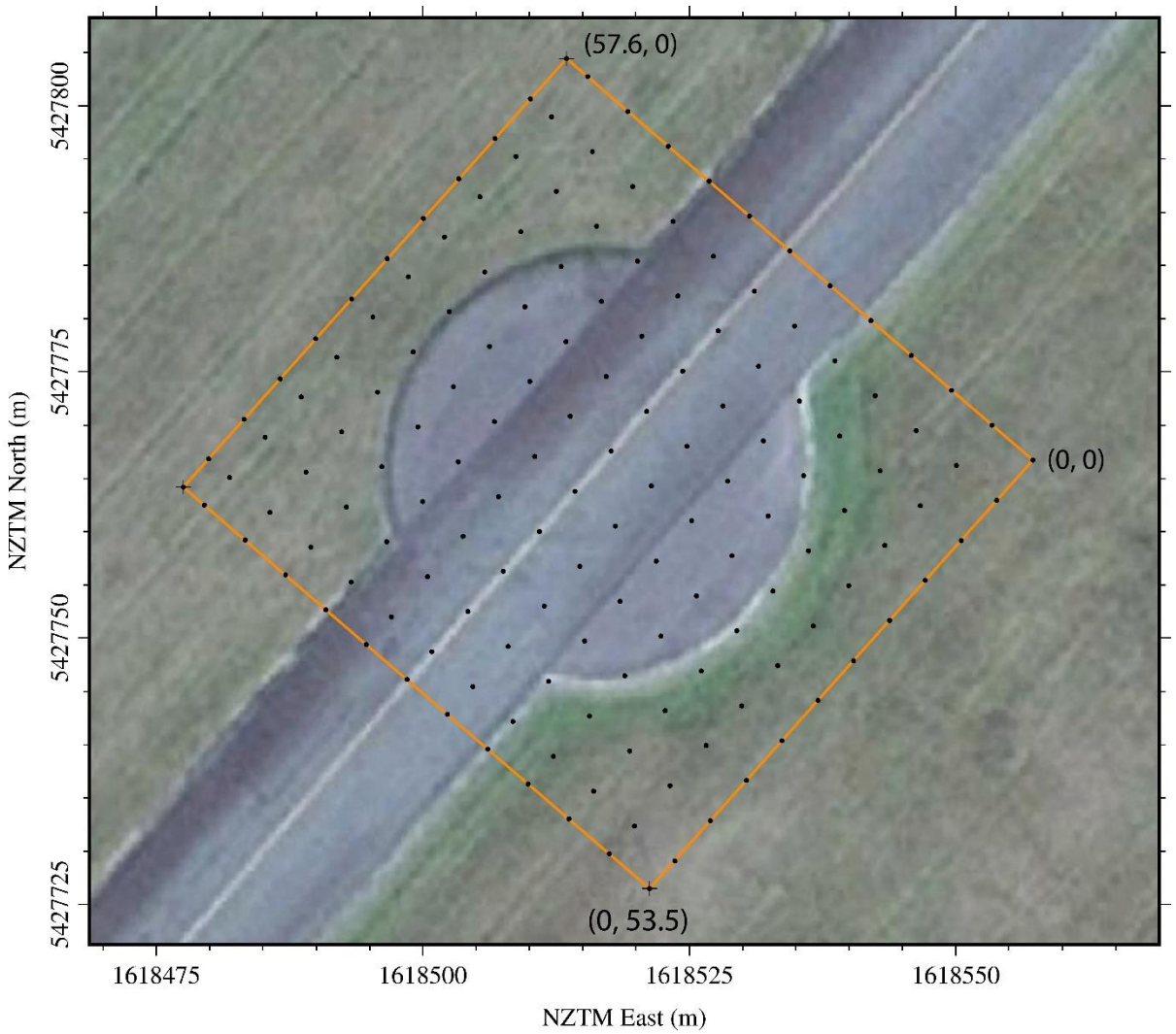

Figure 1. Southern end of the Nelson Airport taxiway showing the compass swing testing site (orange outline), the coordinates of the survey grid, and TF measurement points. Image courtesy of Google Earth, re-projected to the New Zealand Transverse Mercator (NZTM) coordinate system (modified from Benson and Dimech, 2012).

3.1. Equipment

The survey was conducted using a GSM-19TW proton precession magnetometer manufactured by GEM Systems Inc. of Ontario, Canada. This instrument measures Total Magnetic Field Intensity (*TF*) to a precision of ± 0.1 nanoteslas (nT). In practice, the accuracy of an individual reading is ± ~1.0 nT, depending on local geomagnetic conditions.

The instrument's sensor was mounted on top of a 2.24 m pole to filter out potential magnetic anomalies produced by small ferromagnetic objects at or near the ground surface (e.g. a metal nail or a pebble of magnetite-bearing igneous rock). Such anomalies, if present, are only detectable at very short distances and therefore do not affect the operation of a compass swing testing site, since aircraft magnetic sensors are typically at a height that is at least the length of the pole.

3.2. Time-varying components of the geomagnetic field

Short-lived variations in the observed geomagnetic field are generally caused by interactions between the solar wind and the earth's magnetic field. Temporal variations are of concern for a geomagnetic survey because they may introduce false magnetic gradients that exceed the maximum permissible *TF* variation described in AC43-7. The most significant such effect is the diurnal variation that occurs as the angle of the sun changes throughout a day. A correction for the maximum diurnal variation has been applied to the survey data (see Appendix II).

Random large-scale variations in the geomagnetic field are generally the result of solar activity and can persist for several days. The US National Oceanic and Atmospheric Administration reports that there were no geomagnetic storms during the survey period. Furthermore, the 1-minute averaged magnetic observations from the New Zealand Magnetic Observatory at Eyrewell, North Canterbury, show no evidence for any significant geomagnetic events. Short period fluctuations of ~1 nT are a ubiquitous feature of the geomagnetic field; these random variations are difficult to remove and limit the practical resolution of *TF* measurements to ± 1.5 nT.

4. Results

This survey focused on small-scale variation in the geomagnetic field within a relatively small area. Therefore, the mean observed *TF* was subtracted from all diurnal-corrected measurements to obtain residual *TF* anomaly data. The residual *TF* anomaly data are displayed as a contour map in Figure 2 and tabulated in Appendix I.

The total change in residual *TF* anomaly across the site was 8.06 nT, and the data have a near normal distribution around the median (Figure 3). This distribution indicates that the observed geomagnetic field has a single underlying value, and that deviations from this value are the result of two randomly distributed factors: (1) tiny variations in magnetic susceptibility of real earth materials, and (2) measurement uncertainties.

Other than two patches of relatively small positive *TF* anomalies that occur where a trench filled with dark basaltic rock borders the north-western side of the turning circle (see section 4.2), there are no obvious features in the data that would suggest the presence of significant contaminating magnetic material. Small variations in *TF* anomaly (Figure 2) coincide with the order in which the data were collected (traversing along the SE-NW grid lines) and therefore may simply reflect time-varying changes (i.e. random "wobbles") in the geomagnetic field that were not fully removed from the data. From a qualitative perspective, the compass swing testing site is as magnetically quiet as could reasonably be expected from an urban environment.

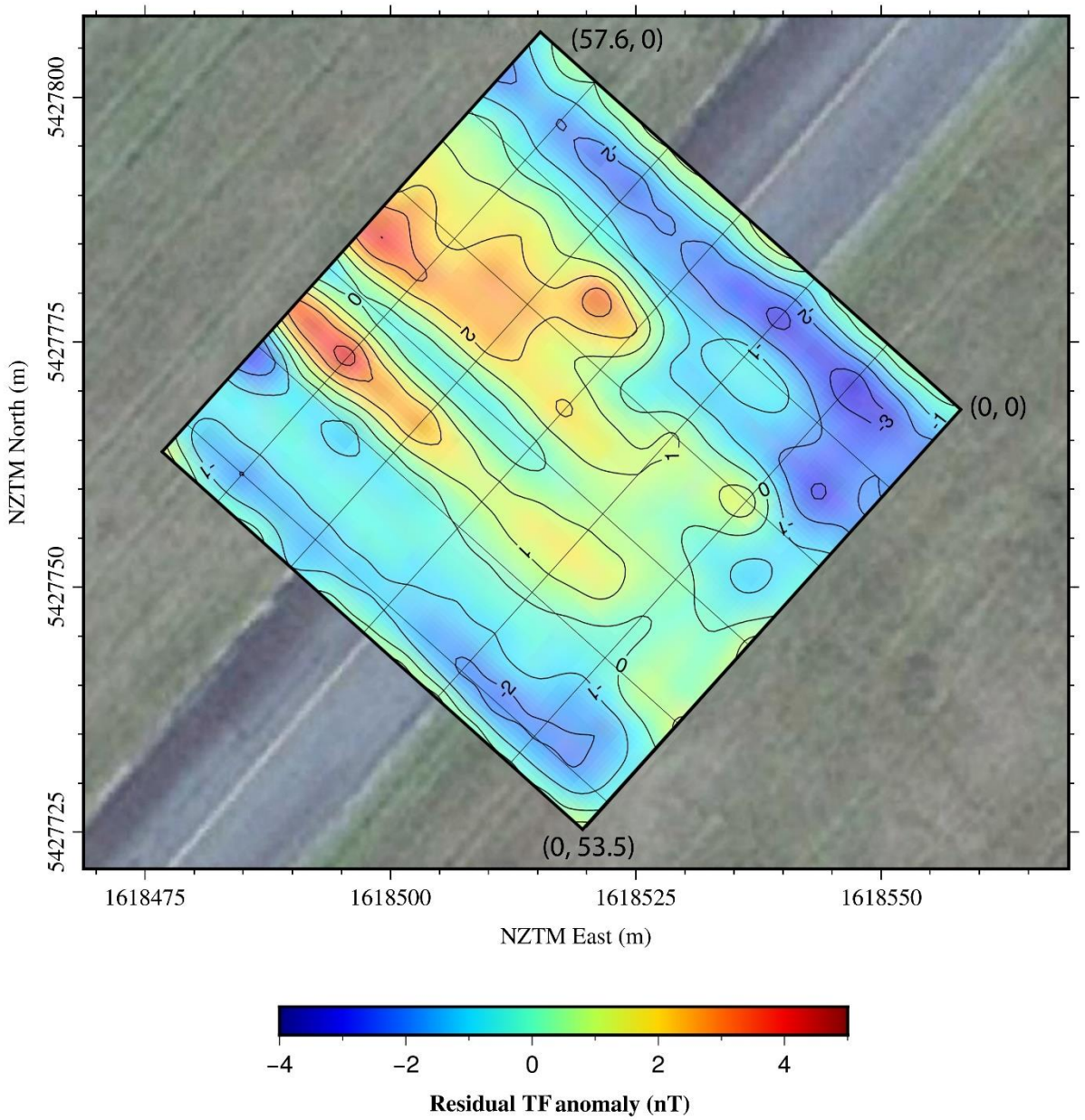

Figure 2. Contour map of residual TF anomaly across the compass swing testing area. Background image courtesy of Google Earth, re-projected to the NZTM coordinate system.

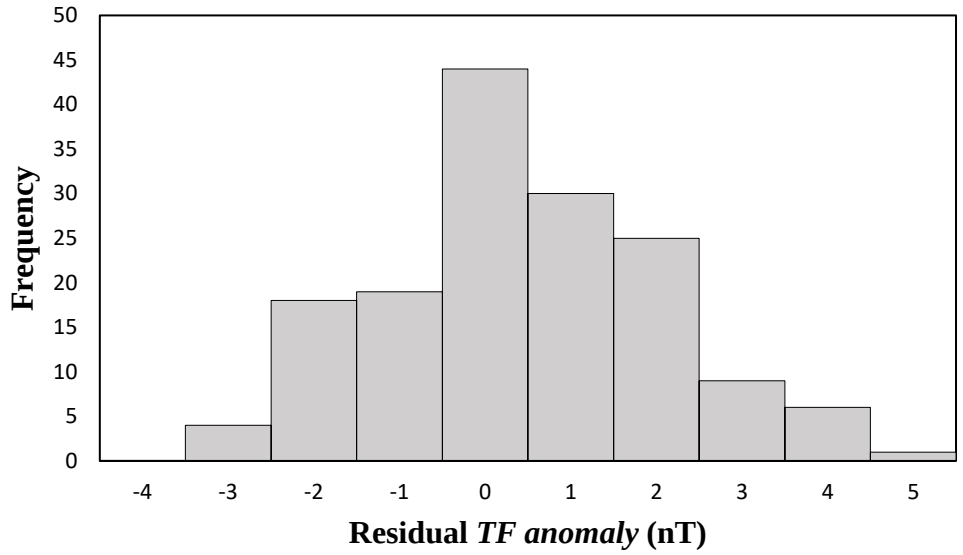

Figure 3. Distribution of residual TF anomaly data.

4.1. Conformance with requirements for Class 1 compass swing testing site

The principal requirement for a suitable compass swing testing site is that the direction of magnetic North (*N*) be stable across the testing area. AC43-7 defines a Class 1 site as one where *N* varies by less than 0.1°. A *TF* survey cannot directly measure deflection of *N*, however a threshold "worst case" change in *TF* (referred to hereafter as δTF_{max}) can be estimated from the following equation:

$$\delta TF_{max} = 0.858 F_{hmax} \sin(0.1°) \sin(I) \qquad (1)$$

where F_{hmax} is the magnitude of the horizontal component of earth's magnetic field, and I is the inclination of earth's magnetic field (CAA, 2000).

Using the values listed in Table 1 (Thébault et al., 2015) we determined a threshold δTF_{max} of 30.4 nT that could disrupt *N* by a maximum of 0.1°. The measured δTF across the site was 8.06 nT, or 26% of the calculated δTF_{max}, which equates to a maximum possible horizontal deflection of *N* by 0.026° for the Nelson Airport compass swing testing site. This is well within the requirements for a Class 1 site.

Date	Declination	Inclination (*I*)	F_{Hmax}	F_{Total}
02.07.2019	22.646°	-66.862	22129 nT	56316 nT

Table 1. International Geomagnetic Reference Field (Generation 12) values for the Nelson Airport compass swing testing site (41.3014°S, 173.2211°E).

4.2. Considerations for maintaining Class 1 status in the future

Since the initial magnetic survey in 2007, Nelson Airport has performed two notable construction works to the testing site. We would like to discuss the effects of such works on the overall *TF* distribution and draw attention to potential consequences of any future construction work at the site. The risks of introducing materials such as pipes or electrical cabling are obvious, however, construction gravel or aggregate may also contain magnetically susceptible materials that could contaminate the site. The Nelson region contains rocks that are known to have strong magnetic properties (Hunt, 1978; Sutherland, 1996); thus, aggregate materials, which are generally quarried locally, may be a source of magnetic contamination.

Between the initial 2007 survey and the resurvey in 2012, Nelson Airport expanded the compass swing testing site by adding a tarmac turning circle. This addition had minimal impact on the total change in *TF* across the site, but the geographic distribution of *TF* anomaly across the testing site changed drastically as a result of this construction (Figure 4a).

In 2019, a ~1 m wide rock-filled trench drain was added that runs along the north-western border of the runway and tarmac turning circle (Figure 4b). The effects of this addition can be seen in the residual *TF* anomaly data of the 2019 resurvey, with the strongest magnetic anomalies occurring at measurement points that were on or near the rocks. This result indicates that the aggregate rocks used to construct the drain contain magnetic minerals.

In the event of any further development of the site, care should be taken to ensure that aggregate materials are not a source of magnetic contamination.

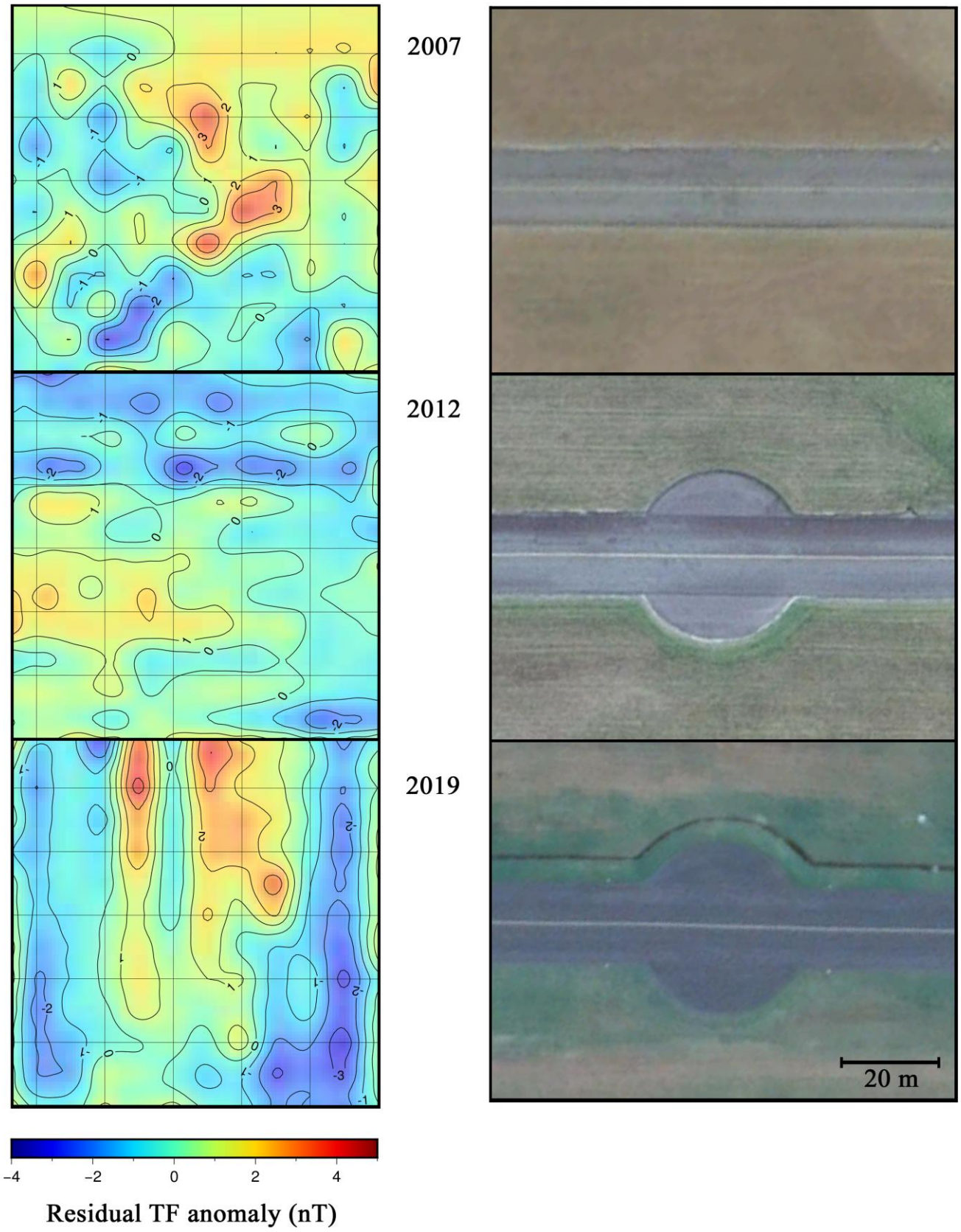

Figure 4a (left). Contour maps of residual TF anomaly across the compass swing testing site over 12 years; grid spacing is 5 metres. Figure 4b (right). Development of the compass swing testing site over 12 years. Aerial runway images courtesy of Google Earth.

5. Conclusions

- A survey of Total Magnetic Field Intensity (*TF*) was conducted across the compass swing testing site at Nelson Airport.
- There are no significant anomalous magnetic features within the site.
- Residual *TF* anomaly varied by 8.06 nT across the site, equivalent to a maximum possible deviation of magnetic North (*N*) by 0.026°.
- The observed *TF* variations are well within the permissible 0.1° deviation of *N* for a Class 1 compass swing testing site as defined in the Civil Aviation Authority Advisory Circular AC43-7 Revision 1.
- The Nelson Airport compass swing testing site maintains its rating as a Class 1 site.

6. References

Benson, A., & Dimech, J. (2012). Geomagnetic survey of the compass swing site at Nelson Airport. Unpublished report.

Civil Aviation Authority of New Zealand (2000). Calibration of compasses and surveying compass swing sites, *Advisory Circular, AC43(7),* 24p.

Henderson, C. M., & Bourguignon, S. (2007). Survey of proposed compass swing site at Nelson Airport. Victoria University of Wellington, 14p.

Hunt, T. (1978), Stokes magnetic anomaly system, *New Zealand Journal of Geology and Geophysics*, 21:5, 595-606, doi: 10.1080/00288306.1978.10424087.

National Oceanic and Atmospheric Administration NOAA (2019), *Solar and Geophysical Activity Summary, 0702SGAS and 0703SGAS.* Downloaded from: ftp://ftp.swpc.noaa.gov/pub/forecasts/SGAS/0702SGAS.txt ftp://ftp.swpc.noaa.gov/pub/forecasts/SGAS/0703SGAS.txt

Sutherland, R. (1996), Magnetic anomalies in the New Zealand region, 1:4,000,000. Lower Hutt: *Institute of Geological & Nuclear Sciences*. Institute of Geological & Nuclear Sciences geophysical map 9(1) map.

Thébault, E. et al. (2015), International Geomagnetic Reference Field: the 12th generation, *Earth, Planets and Space*, 67, 79, doi: 10.1186/s40623-015-0228-9.

7. Acknowledgments

During the preparation of this report we used data collected from the New Zealand Magnetic Observatory at Eyrewell. We thank GNS Science for supporting its operation and INTERMAGNET for promoting high standards of Magnetic observatory practice (www.intermagnet.org).

Appendix I. Survey data

Local Grid (m)		**Observation Time (UTC)**		**Total Magnetic Field (nT)**		
x	*y*	*DD-MM-YYYY*	*hh:mm:ss*	*Observed*	*Diurnal Corrected*	*Anomaly*
0.0	0.0	01-07-2019	23:44:59.9	56481.21	56481.21	-0.17
5.0	0.0	01-07-2019	23:46:02.8	56481.93	56481.92	0.54
10.0	0.0	01-07-2019	23:46:56.2	56481.96	56481.95	0.56
15.0	0.0	01-07-2019	23:48:07.2	56481.72	56481.70	0.32
20.0	0.0	01-07-2019	23:48:46.3	56480.96	56480.94	-0.45
25.0	0.0	01-07-2019	23:49:16.1	56482.99	56482.96	1.58
30.0	0.0	01-07-2019	23:49:49.8	56482.23	56482.20	0.82
35.0	0.0	01-07-2019	23:50:32.8	56482.39	56482.35	0.97
40.0	0.0	01-07-2019	23:51:03.0	56482.49	56482.45	1.07
45.0	0.0	01-07-2019	23:51:36.9	56482.17	56482.13	0.74
50.0	0.0	01-07-2019	23:52:17.2	56481.46	56481.41	0.03
55.0	0.0	01-07-2019	23:53:50.7	56481.73	56481.67	0.29
57.6	0.0	01-07-2019	23:54:30.2	56480.80	56480.74	-0.64
0.0	0.0	01-07-2019	23:56:15.7	56480.95	56480.95	-0.43
0.0	5.0	01-07-2019	23:56:49.4	56479.03	56478.97	-2.41
5.0	5.0	01-07-2019	23:57:16.5	56478.44	56478.33	-3.05
10.0	5.0	01-07-2019	23:57:46.7	56477.94	56477.78	-3.61
15.0	5.0	01-07-2019	23:58:14.5	56478.69	56478.47	-2.91
20.0	5.0	01-07-2019	23:58:37.5	56478.31	56478.06	-3.33
25.0	5.0	01-07-2019	23:59:08.8	56478.88	56478.57	-2.81
30.0	5.0	01-07-2019	23:59:37.3	56479.42	56479.06	-2.32
35.0	5.0	02-07-2019	00:00:04.1	56479.71	56479.30	-2.08
40.0	5.0	02-07-2019	00:00:33.3	56479.19	56478.73	-2.66
45.0	5.0	02-07-2019	00:01:39.8	56479.45	56478.87	-2.51
50.0	5.0	02-07-2019	00:02:38.4	56480.02	56479.33	-2.05
55.0	5.0	02-07-2019	00:03:25.8	56480.27	56479.50	-1.88
57.6	5.0	02-07-2019	00:03:46.6	56479.93	56479.12	-2.26
0.0	0.0	02-07-2019	00:04:59.7	56480.01	56480.01	-1.37
0.0	10.0	02-07-2019	00:05:57.1	56479.06	56479.12	-2.26
5.0	10.0	02-07-2019	00:07:50.1	56478.64	56478.82	-2.56
10.0	10.0	02-07-2019	00:08:40.0	56479.26	56479.50	-1.88
15.0	10.0	02-07-2019	00:09:35.7	56480.33	56480.63	-0.75
20.0	10.0	02-07-2019	00:10:27.3	56480.57	56480.93	-0.46
25.0	10.0	02-07-2019	00:11:17.2	56479.63	56480.04	-1.34
30.0	10.0	02-07-2019	00:11:42.4	56479.66	56480.10	-1.29
35.0	10.0	02-07-2019	00:13:00.3	56479.90	56480.42	-0.96
40.0	10.0	02-07-2019	00:13:31.5	56480.49	56481.04	-0.34
45.0	10.0	02-07-2019	00:14:18.3	56480.64	56481.25	-0.14
50.0	10.0	02-07-2019	00:14:41.6	56480.31	56480.94	-0.44
55.0	10.0	02-07-2019	00:15:54.2	56480.95	56481.66	0.28
57.6	10.0	02-07-2019	00:16:13.8	56480.53	56481.26	-0.12

Local Grid (m)		**Observation Time (UTC)**		**Total Magnetic Field (nT)**		
x	*y*	*DD-MM-YYYY*	*hh:mm:ss*	*Observed*	*Diurnal Corrected*	*Anomaly*
0.0	0.0	01-07-2019	00:17:26.7	56480.82	56480.82	-0.56
0.0	15.0	01-07-2019	00:18:14.5	56479.17	56479.18	-2.20
5.0	15.0	01-07-2019	00:18:52.1	56478.21	56478.24	-3.15
10.0	15.0	01-07-2019	00:19:30.8	56479.25	56479.29	-2.10
15.0	15.0	01-07-2019	00:19:59.8	56479.91	56479.96	-1.43
20.0	15.0	01-07-2019	00:20:29.7	56479.97	56480.02	-1.36
25.0	15.0	01-07-2019	00:21:18.5	56480.29	56480.36	-1.02
30.0	15.0	01-07-2019	00:44:12.8	56482.98	56483.46	2.08
35.0	15.0	01-07-2019	00:44:56.3	56484.52	56485.01	3.63
40.0	15.0	01-07-2019	00:45:33.5	56482.19	56482.69	1.31
45.0	15.0	01-07-2019	00:45:57.5	56482.77	56483.28	1.90
50.0	15.0	01-07-2019	00:46:36.9	56482.28	56482.80	1.42
55.0	15.0	01-07-2019	00:46:59.2	56481.97	56482.50	1.12
57.6	15.0	01-07-2019	00:47:20.8	56482.05	56482.59	1.20
0.0	0.0	01-07-2019	00:48:40.2	56481.38	56481.38	-0.00
0.0	20.0	01-07-2019	00:49:27.9	56480.69	56480.78	-0.61
5.0	20.0	01-07-2019	00:49:54.4	56480.38	56480.51	-0.87
10.0	20.0	01-07-2019	00:51:17.8	56482.66	56482.94	1.56
15.0	20.0	01-07-2019	00:52:16.3	56481.68	56482.07	0.69
20.0	20.0	01-07-2019	00:52:37.4	56482.06	56482.49	1.10
25.0	20.0	01-07-2019	00:53:11.9	56480.66	56481.15	-0.23
30.0	20.0	01-07-2019	00:53:37.6	56481.45	56481.99	0.60
35.0	20.0	01-07-2019	00:54:01.3	56482.29	56482.87	1.48
40.0	20.0	01-07-2019	00:54:24.5	56483.54	56484.16	2.78
45.0	20.0	01-07-2019	00:55:07.0	56483.64	56484.34	2.95
50.0	20.0	01-07-2019	00:55:28.9	56482.52	56483.26	1.87
55.0	20.0	01-07-2019	00:56:19.2	56483.28	56484.11	2.72
57.6	20.0	01-07-2019	00:57:05.1	56482.27	56483.18	1.80
0.0	0.0	01-07-2019	00:58:12.3	56482.41	56482.41	1.03
0.0	25.0	01-07-2019	00:59:16.5	56481.04	56481.14	-0.24
5.0	25.0	02-07-2019	01:00:15.6	56479.92	56480.12	-1.27
10.0	25.0	02-07-2019	01:00:46.3	56480.78	56481.03	-0.36
15.0	25.0	02-07-2019	01:01:44.5	56481.33	56481.67	0.29
20.0	25.0	02-07-2019	01:02:16.9	56481.99	56482.38	0.10
25.0	25.0	02-07-2019	01:02:53.5	56482.62	56483.07	1.69
30.0	25.0	02-07-2019	01:03:19.1	56483.07	56483.56	2.18
35.0	25.0	02-07-2019	01:03:56.9	56482.71	56483.26	1.88
40.0	25.0	02-07-2019	01:04:24.8	56483.37	56483.97	2.58
45.0	25.0	02-07-2019	01:04:48.4	56483.22	56483.85	2.47
50.0	25.0	02-07-2019	01:05:07.7	56483.85	56484.52	3.13
55.0	25.0	02-07-2019	01:05:30.7	56484.64	56485.34	3.96
57.6	25.0	02-07-2019	01:05:49.0	56484.30	56485.03	3.65
0.0	0.0	02-07-2019	01:07:22.0	56483.29	56483.29	1.91
0.0	30.0	02-07-2019	01:08:04.7	56482.99	56482.79	1.40

Local Grid (m)		**Observation Time (UTC)**		**Total Magnetic Field (nT)**		
x	*y*	*DD-MM-YYYY*	*hh:mm:ss*	*Observed*	*Diurnal Corrected*	*Anomaly*
5.0	30.0	02-07-2019	01:08:25.7	56481.53	56481.23	-0.15
10.0	30.0	02-07-2019	01:08:58.4	56482.31	56481.85	0.47
15.0	30.0	02-07-2019	01:09:26.9	56482.77	56482.18	0.80
20.0	30.0	02-07-2019	01:09:49.2	56482.81	56482.11	0.73
25.0	30.0	02-07-2019	01:10:09.8	56482.43	56481.64	0.25
30.0	30.0	02-07-2019	01:10:46.6	56481.99	56481.02	-0.36
35.0	30.0	02-07-2019	01:11:09.6	56481.88	56480.80	-0.58
40.0	30.0	02-07-2019	01:12:12.2	56482.00	56480.63	-0.76
45.0	30.0	02-07-2019	01:13:00.7	56482.34	56480.74	-0.64
50.0	30.0	02-07-2019	01:13:24.3	56482.68	56480.97	-0.42
55.0	30.0	02-07-2019	01:14:04.4	56483.00	56481.10	-0.29
57.6	30.0	02-07-2019	01:14:24.7	56482.57	56480.57	-0.81
0.0	0.0	02-07-2019	01:15:34.8	56480.96	56480.96	-0.42
0.0	35.0	02-07-2019	01:16:34.6	56481.67	56482.07	0.69
5.0	35.0	02-07-2019	01:16:56.9	56481.27	56481.83	0.44
10.0	35.0	02-07-2019	01:17:19.4	56480.64	56481.35	-0.03
15.0	35.0	02-07-2019	01:17:47.1	56481.96	56482.86	1.47
20.0	35.0	02-07-2019	01:18:07.1	56482.12	56483.15	1.77
25.0	35.0	02-07-2019	01:18:25.4	56481.88	56483.04	1.65
30.0	35.0	02-07-2019	01:18:57.9	56481.23	56482.61	1.22
35.0	35.0	02-07-2019	01:19:22.6	56481.63	56483.17	1.79
40.0	35.0	02-07-2019	01:19:44.1	56482.66	56484.35	2.96
45.0	35.0	02-07-2019	01:20:02.7	56482.53	56484.34	2.96
50.0	35.0	02-07-2019	01:20:26.3	56483.86	56485.83	4.45
55.0	35.0	02-07-2019	01:20:46.1	56483.22	56485.33	3.94
57.6	35.0	02-07-2019	01:21:05.3	56482.50	56484.74	3.35
0.0	0.0	02-07-2019	01:22:23.9	56483.75	56483.75	2.37
0.0	40.0	02-07-2019	01:23:19.4	56482.79	56482.54	1.15
5.0	40.0	02-07-2019	01:23:50.4	56482.63	56482.24	0.85
10.0	40.0	02-07-2019	01:24:10.4	56481.42	56480.94	-0.45
15.0	40.0	02-07-2019	01:24:30.2	56481.73	56481.16	-0.23
20.0	40.0	02-07-2019	01:24:56.8	56482.31	56481.62	0.23
25.0	40.0	02-07-2019	01:25:35.5	56482.43	56481.56	0.18
30.0	40.0	02-07-2019	01:25:56.5	56482.40	56481.43	0.05
35.0	40.0	02-07-2019	01:26:38.8	56481.92	56480.76	-0.62
40.0	40.0	02-07-2019	01:27:03.1	56481.86	56480.59	-0.79
45.0	40.0	02-07-2019	01:27:24.3	56481.49	56480.13	-1.26
50.0	40.0	02-07-2019	01:27:43.9	56482.08	56480.63	-0.76
55.0	40.0	02-07-2019	01:28:01.8	56480.98	56479.45	-1.94
57.6	40.0	02-07-2019	01:28:19.3	56480.17	56478.56	-2.83
0.0	0.0	02-07-2019	01:29:53.3	56481.71	56481.71	0.33
0.0	45.0	02-07-2019	01:30:51.2	56480.78	56480.77	-0.62
5.0	45.0	02-07-2019	01:31:12.5	56479.53	56479.51	-1.87
10.0	45.0	02-07-2019	01:31:37.7	56479.70	56479.68	-1.71

Local Grid (m)		**Observation Time (UTC)**		**Total Magnetic Field (nT)**		
x	*y*	*DD-MM-YYYY*	*hh:mm:ss*	*Observed*	*Diurnal Corrected*	*Anomaly*
15.0	45.0	02-07-2019	01:32:37.3	56480.73	56480.69	-0.69
20.0	45.0	02-07-2019	01:33:00.5	56480.47	56480.43	-0.96
25.0	45.0	02-07-2019	01:33:28.9	56480.49	56480.44	-0.94
30.0	45.0	02-07-2019	01:34:03.1	56480.57	56480.51	-0.87
35.0	45.0	02-07-2019	01:34:26.0	56480.99	56480.93	-0.45
40.0	45.0	02-07-2019	01:34:53.1	56481.01	56480.94	-0.44
45.0	45.0	02-07-2019	01:35:16.5	56480.97	56480.90	-0.49
50.0	45.0	02-07-2019	01:35:55.7	56481.04	56480.96	-0.42
55.0	45.0	02-07-2019	01:36:18.2	56480.89	56480.80	-0.58
57.6	45.0	02-07-2019	01:36:38.7	56480.88	56480.79	-0.59
0.0	0.0	02-07-2019	01:38:04.4	56481.60	56481.60	0.22
0.0	50.0	02-07-2019	01:39:37.9	56481.01	56481.05	-0.33
5.0	50.0	02-07-2019	01:39:59.2	56479.37	56479.42	-1.96
10.0	50.0	02-07-2019	01:41:27.8	56479.23	56479.32	-2.06
15.0	50.0	02-07-2019	01:42:13.8	56478.89	56479.00	-2.38
20.0	50.0	02-07-2019	01:42:33.7	56479.14	56479.26	-2.12
25.0	50.0	02-07-2019	01:43:00.3	56479.50	56479.64	-1.75
30.0	50.0	02-07-2019	01:43:19.7	56480.09	56480.24	-1.15
35.0	50.0	02-07-2019	01:43:39.1	56479.88	56480.03	-1.35
40.0	50.0	02-07-2019	01:43:58.7	56479.60	56479.76	-1.62
45.0	50.0	02-07-2019	01:44:21.2	56479.52	56479.69	-1.69
50.0	50.0	02-07-2019	01:44:40.7	56479.16	56479.34	-2.04
55.0	50.0	02-07-2019	01:45:03.1	56479.58	56479.77	-1.61
57.6	50.0	02-07-2019	01:45:20.9	56480.49	56480.69	-0.69
0.0	0.0	02-07-2019	01:46:45.2	56481.84	56481.84	0.46
0.0	53.5	02-07-2019	01:48:38.4	56483.06	56483.19	1.80
5.0	53.5	02-07-2019	01:48:59.7	56481.56	56481.71	0.33
10.0	53.5	02-07-2019	01:49:19.2	56481.42	56481.59	0.21
15.0	53.5	02-07-2019	01:49:49.8	56481.92	56482.13	0.74
20.0	53.5	02-07-2019	01:50:14.7	56482.50	56482.74	1.35
25.0	53.5	02-07-2019	01:50:34.8	56482.46	56482.72	1.34
30.0	53.5	02-07-2019	01:50:53.1	56481.59	56481.87	0.49
35.0	53.5	02-07-2019	01:51:11.5	56481.54	56481.84	0.46
40.0	53.5	02-07-2019	01:51:38.9	56480.07	56480.40	-0.98
45.0	53.5	02-07-2019	01:52:03.4	56481.54	56481.90	0.51
50.0	53.5	02-07-2019	01:52:21.9	56480.94	56481.32	-0.06
55.0	53.5	02-07-2019	01:52:46.7	56481.84	56482.25	0.86
57.6	53.5	02-07-2019	01:53:06.6	56482.57	56482.10	1.61
0.0	0.0	02-07-2019	01:54:53.9	56482.94	56482.94	1.56

Appendix II. Correction for temporal variations in the geomagnetic field

Repeated measurements made at the base station [grid point (0, 0)] are tabulated below. *TF* varied by up to 3.74 nT over the course of the survey, approximately half of the total observed *TF* anomaly.

A diurnal correction was applied to each reading of the survey by interpolating the base station value at the time of measurement (Figure AII.1) and then subtracting the interpolated value from the reading. It should be noted that any magnetic field fluctuations occurring during the intervals between base station readings cannot be resolved and therefore are not removed from the survey data.

Observation Time (UTC)		**Total Magnetic Field**
DD-MM-YYYY	*hh:mm:ss*	**(nT)**
01-07-2019	23:44:59.9	56481.21
01-07-2019	23:56:15.7	56480.95
02-07-2019	00:04:59.7	56480.01
02-07-2019	00:17:26.7	56480.82
02-07-2019	00:48:40.2	56481.38
02-07-2019	00:58:12.3	56482.41
02-07-2019	01:07:22.0	56483.29
02-07-2019	01:15:34.8	56480.96
02-07-2019	01:22:23.9	56483.75
02-07-2019	01:29:53.3	56481.71
02-07-2019	01:38:04.4	56481.60
02-07-2019	01:46:45.2	56481.84
02-07-2019	01:54:53.9	56482.39

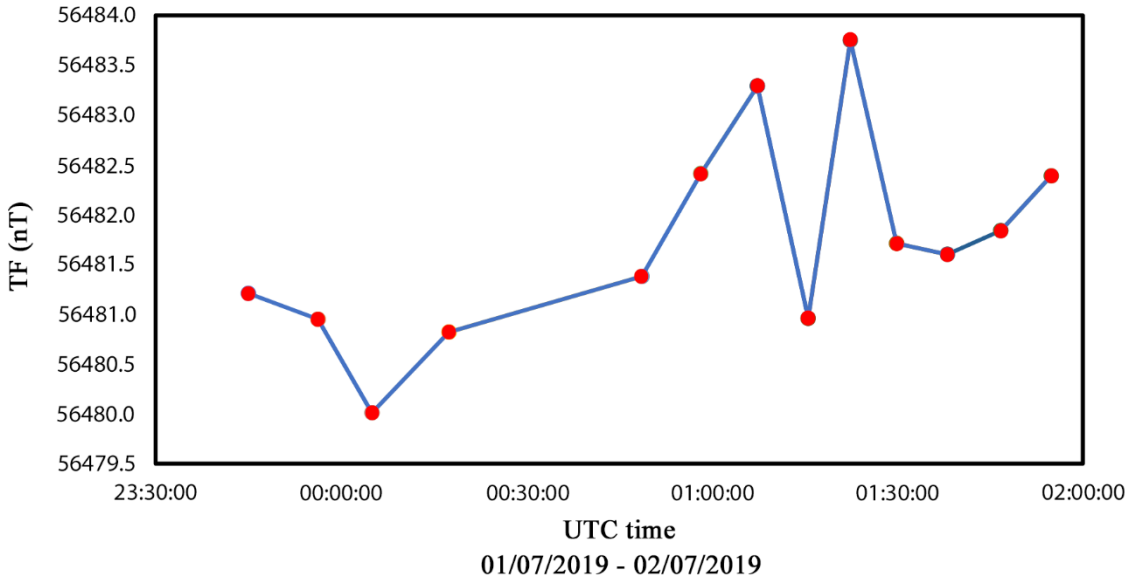

Figure AII.1. Diurnal variation as seen by TF measurements at grid point (0, 0).